Journal of the Korean Nuclear Society
Volume 30, Number 6, pp.581~591, December 1998

Evaluation of Thermal Stratification Effect in a Long Horizontal Pipeline with Turbulent Natural Convection

Man-Heung Park
Korea Power Engineering Company, Inc.,
369-9 Mabuk-ri, Kusung-myon, Yongin-shi, Kyunggi-do, Korea

Jang-Sun Ahn, Seung-Deog Nam
Korea Power Engineering Company, Inc.,
150 Dukjin-dong, Yusong-gu, Taejon 305-353, Korea

(Received March 27, 1998)

Abstract

Numerical analysis was performed for the two-dimensional turbulent natural convection for a long horizontal line with different end temperatures. The turbulent model has been applied a standard k-ε two equation model of turbulence similar to that the proposed by the Launder and Spalding. The dimensionless governing equations are solved by using SIMPLE (Semi-Implicit Method for Pressure Linked Equations) algorithm which is developed using control volumes and staggered grids. The numerical results are verified by comparison with the operating PWR test data. The analysis focuses on the effects of variation of the heat transfer rates at the pipe surface, the thermal conductivities of the pipe material and the thickness of the pipe wall on the thermal stratification. The results show that the heat transfer rate at the pipe surface is the controlling parameter for mitigating of thermal stratification in the long horizontal pipe. A significant reduction and disappearance of the thermal stratification phenomenon is observed at the Biot number of 4.82×10^{-1}. The results also show that the increment of the thermal conductivity and thickness of the wall weakens a little the thermal stratification and somewhat reduces temperature gradient of y-direction in the pipe wall. These effects are however minor, when compared with those due to the variation of the heat transfer rates at the surface of the pipe wall.

1. Introduction

Natural convection in long horizontal lines with different end temperatures can result in thermal stratification of the fluid. Thermal stratification in the light water nuclear reactor (LWR) piping systems has recently been considered as the subject of safety concerns. The phenomenon of thermal stratification plays an important role in the piping integrity, because the significant thermal stresses may induce the failure and the unexpected

deformation of the piping lines of PWR plant[1,2]. Since then, the thermal stresses resulting in the stratification of the hot and cold fluids have been considered by the utilities and vendors for the design and licensing processes of piping. As a result, these pipes of the PWR have been recently designed using the results of thermal stress.

The stability of the flow stratification is dependent on the differences in temperature and velocity of the flow. Greater temperature differences and lower velocities result in more stable stratification conditions. The Richardson number gives a measure of the stability of a stratified flow. It is a dimensionless parameter representing a ratio of buoyancy force to inertia force. If the Richardson number exceeds unity, the stratification may be stable. If the Richardson number is less than unity, the stratification is unstable and may become unstratified. Stratified flow is generated under a condition in which hotter fluid flows over a colder region of fluid.

Hong[3] has studied numerically natural circulations in a horizontal pipe. Bejan and Tien[4] have modeled for the thermal-hydraulic aspects of stratified flow. Kimura and Bejan[5] have found that the flow is characterized by heat transfer through the boundary layers at the hot and cold ends connected by a fully developed flow in the core region. Shiralkar and Tien[6] have investigated high Rayleigh number convection in shallow enclosures with different end temperatures.

Lubin and Kim[7] have developed a model to predict the wall temperatures in long horizontal lines with different end temperatures undergoing natural convection at very high Rayleigh number. Lubin and Brown[8] have treated the thermal stratification in a line connected to a reactor coolant system as the pin model

For a horizontal circular cylinder, Farouk[9] has employed the standard k-ϵ model to obtain numerical solution of the turbulent natural convection. Park and Lee[10] have performed an turbulent natural convection flow and heat transfer in an inclined square enclosure.

The existing analysis have only been studied in viewpoint of the heat transfer and fluid flow in a horizontal pipe with thermal stratification.

The purpose of this study is to investigate the controlling parameter for mitigating and preventing of thermal stratification of the flow in a horizontal pipeline through a numerical analysis and to suggest a feasible design changes to mitigate thermal stratification in the safety injection line of the PWR plant. In the horizontal piping design expected thermal stratification, the mainly considering parameters are the piping material specifications and the piping thermal conditions. The effective parameters of piping material specifications are the thermal conductivity of piping and the piping thickness. And, the effective parameter of thermal conditions is the heat transfer coefficient of the piping outside surface if the piping outside temperature is constant. Therefore, the analysis is focused on the effects of variation of the heat transfer rates at the pipe surface, the thermal conductivities and the thickness of the pipe wall on the thermal stratification in the long pipeline.

The phenomena of turbulent natural convection with thermal stratification in enclosure have been investigated numerically with standard k-ϵ turbulent model. Also, this study have been performed for the heat transfer and flow characteristics in a long horizontal line (the safety injection line) with different end temperatures undergoing natural convection at very high Rayleigh number.

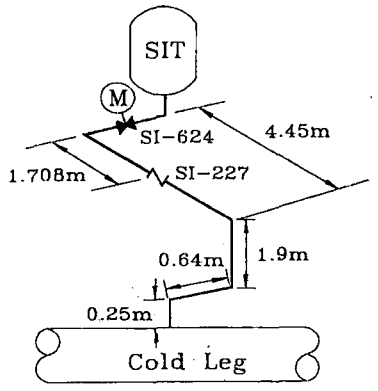

Fig. 1. Isometric Diagram on the Safety Injection Line of PWR Plant of CE Type

2. Model Formulation

2.1. Physical Phenomena

The safety injection line connects the safety injection tanks to the cold leg of the reactor coolant system of CE type as shown in Fig.1. The line runs from a safety injection nozzle, oriented in a vertical up position on the cold leg of the RCS. Typical lines have one or more long horizontal sections between vertical rises. Line size is 0.34 m nominal diameter and schedule of 160.

In normal operation, the safety injection (SI) line is isolated from the cold leg by a check valve that is normally closed. And the motor operated valve, that is used to isolate the safety injection tank, is open. However, during plant heatup, cooldown and refueling operation, the motor operated valve is closed to prevent the injection of SIT fluid to reactor coolant system. The fluid temperature of RCS is varied from 38℃ at cold shutdown to full power operation. But fluid in the safety injection tanks is typically maintained about 38℃ as containment temperature.

In general, wall temperatures between the RCS and the check valve is close to the RCS temperatures and indicate small variation with angular location. However, those between the check valve and the motor operated valve, while lower than the RCS temperature due to the thermal resistance of valve, have top-to-bottom variations in wall temperature of about higher than 60℃ [8]. Wall temperature distributions were observed to be directly related to RCS temperature. As a result of this and absence of forced flow in the line, the observed wall temperature differences were credited to natural convection between a source of high temperature at the check valve and cold temperature close to the motor operated valve.

2.2. Assumption of Calculation Domain

The large pipe diameter and high temperatures resulted in a Rayleigh number for natural convection on the order of magnitude of 10^{11}. An approximate region map for natural convection in long enclosures shows that natural convection for these Rayleigh numbers falls in what may be termed the "intrusion layer regions"[11].

Practically, pipe shape is three-dimensional cylindrical shape. However, the natural convection flow in long enclosures could be divided into two regions: a boundary layer near the ends and at about the order of magnitude of the plate spacing from the ends(boundary layer region), and a core flow region(intrusion layer region)[11].

The flow is characterized by heat transfer through the boundary layers at the hot and cold ends connected by a fully developed flow in the core region. Specially, in the natural convection by high temperature difference, the circulation flow of enclosure occurs almost near to pipe wall, and then the flow of core region is almost stationary (The thin top and bottom intrusion layers are connected by an almost stationary core). Also, the flow variation of circumferential direction in the

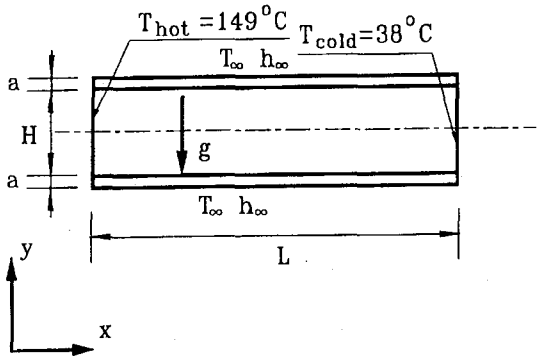

Fig. 2. Schematic Diagram of the Calculation Domain

intrusion layer region(core) is out of existence, but the flow of z-direction occurs strongly and the small scale boundary flow occurs in the vertical wall. The main focus of the this study is to analyse the temperature difference of the bottom and top of pipe core flow region when the thermal stratification exists in the horizontal pipe. Therefore, the calculation domain is assumed to be a rectangular section because the variation of temperature with angular direction is very small in the long horizontal pipe lines. Therefore, we can assume the steady two-dimensional turbulent model for the rectangular enclosure flow[7, 8].

In this study, the calculation domain as Fig. 2 is selected to analyze the stratified flow for cylindrical enclosure. The horizontal pipe length between two valves, L, and the inner diameter of pipe, H, are 1.708 m and 0.284 m, respectively and the wall thickness, a, is 0.028 m. The temperature of hot fluid, T_{hot}, is 149℃ and that of cold fluid, T_{cold}, is 38℃. Also, the ambient temperature is 38℃ and the equivalent heat transfer coefficient of insulated piping, h_∞, is 0.026 W/m^{2}K.

2.3. The Governing Equations

The major assumptions to solve the governing equations are as follows;

a) the fluid flow and the heat transfer of hot and cold fluids is two-dimensional.

b) properties of fluid and solid except density in the body force term are treated as constant.

c) the compressibility effects, viscous dissipation and radiation heat transfer of fluids are neglected.

For this term a linear variation of density with temperature is assumed, according to the following equation.

$$\rho = \rho_o [\, 1 - \beta(T^* - T_o^*) \,] \tag{1}$$

Some simplification of the resulting body force terms is represented by defining an effective pressure, P*.

$$P^* = P + \rho_o g y^* + \frac{2}{3} \rho_o k^* \tag{2}$$

Dimensionless variables are then formed as follows;

$$x = \frac{x^*}{H}, \quad y = \frac{y^*}{H}, \quad a = \frac{a^*}{H},$$

$$u = u^* \frac{H}{\nu}, \quad v = v^* \frac{H}{\nu}, \quad P = \frac{P^* H^2}{\rho_o \nu^2},$$

$$T = \frac{T^* - T^*_{cold}}{T^*_{hot} - T^*_{cold}}, \quad \varepsilon = \varepsilon^* \frac{H^4}{\nu^3}, \quad K = K^* \frac{H^2}{\nu^2}, \tag{3}$$

$$\mu_t = \frac{\mu_t^*}{\mu}, \quad \mathrm{Pr} = \frac{C_p \mu}{k_f}, \quad Bi = \frac{h\, a^*}{k_s},$$

$$Gr = \frac{g \beta H^{*3} (T^*_{hot} - T^*_{cold})}{\nu^2}$$

For a steady two-dimensional flow, the following governing equations represent the conservation of the dimensionless time-averaged quantities. The same two-dimensional standard k-ε model for turbulence as employed by Farouk[9] and Park[10] has been used for present study.

$$\frac{\partial u}{\partial x} + \frac{\partial v}{\partial y} = 0 \tag{4}$$

$$\frac{\partial}{\partial x}(u^2)+\frac{\partial}{\partial y}(uv)= -\frac{\partial P}{\partial x}+\frac{\partial}{\partial x}(\mu_{eff}\frac{\partial u}{\partial x})+\frac{\partial}{\partial y}(\mu_{eff}\frac{\partial u}{\partial y})+S_u \quad (5)$$

$$\frac{\partial}{\partial x}(uv)+\frac{\partial}{\partial y}(v^2)= -\frac{\partial P}{\partial y}+\frac{\partial}{\partial x}(\mu_{eff}\frac{\partial v}{\partial x})+\frac{\partial}{\partial y}(\mu_{eff}\frac{\partial v}{\partial y})+S_v \quad (6)$$

$$\frac{\partial}{\partial x}(u\phi)+\frac{\partial}{\partial y}(v\phi)= \frac{\partial}{\partial x}(\Gamma_{\phi,eff}\frac{\partial \phi}{\partial x})+\frac{\partial}{\partial y}(\Gamma_{\phi,eff}\frac{\partial \phi}{\partial y})+S_\phi \quad (7)$$

Where μ_{eff} ($=\mu_t+1$) is the effective viscosity, and Γ_ϕ is the exchange coefficient for the transport of property ϕ ($= T$, K and ε).

The exchange coefficient of energy, turbulent kinetic energy and rate of dissipation of turbulent energy are $\Gamma_{T,eff}=(\mu_t/\sigma_T)+(1/Pr)$, $\Gamma_{K,eff}=(\mu_t/\sigma_K)+1$ and $\Gamma_{\varepsilon,eff}=(\mu_t/\sigma_\varepsilon)+1$, respectively.

The source term, S, in the governing equations are as follows:

$$S_u=\frac{\partial}{\partial x}(\mu_t\frac{\partial u}{\partial x})+\frac{\partial}{\partial x}(\mu_t\frac{\partial v}{\partial y}) \quad (8)$$

$$S_v=\frac{\partial}{\partial y}(\mu_t\frac{\partial u}{\partial x})+\frac{\partial}{\partial y}(\mu_t\frac{\partial v}{\partial y})+G\gamma T \quad (9)$$

$$S_T=0 \quad (10)$$

$$S_K=G-\varepsilon-B \quad (11)$$

$$S_\varepsilon=\frac{\varepsilon}{k}(C_1G-C_2\varepsilon-C_3B) \quad (12)$$

$$G=\mu_t[2[(\frac{\partial u}{\partial x})^2+(\frac{\partial v}{\partial y})^2]+(\frac{\partial u}{\partial y}+\frac{\partial v}{\partial x})^2] \quad (13)$$

$$B=G\gamma\frac{\mu_t}{\sigma_T}\frac{\partial T}{\partial y} \quad (14)$$

Table 1. The Constant Used in Turbulence Modeling

C_μ	C_1	C_2	C_3	σ_T	σ_K	σ_ε
0.09	1.44	1.92	0.7	1.0	1.0	1.3

$$\mu_t=C_\mu\frac{K^2}{\varepsilon} \quad (15)$$

Numerical values for C_μ, C_1, C_2, C_3, σ_T, σ_K and σ_ε are taken as recommended by Launder and Spalding[12]. The constant C_3 in the buoyancy term of above equation has been adopted from Fraikin et al.[13].

They are given in Table 1.

The following boundary conditions have been used:

$$x=0 \quad ; T=0.0,\ u=v=K=0 \quad (16)$$

$$x=\frac{L}{H};\ T=1.0,\ u=v=K=0 \quad (17)$$

$$y=0,\ 1+2a\ ; \frac{\partial T}{\partial y}=-\frac{Bi}{a}(T_s-T_\infty),\ u=v=K=0 \quad (18)$$

$$y=a,\ 1+2a\ ;\quad k_f\frac{\partial T_f}{\partial y}=k_s\frac{\partial T_s}{\partial y} \quad (19)$$

The time-averaged rate of dissipation of turbulent energy, ε, is proportional to $K^{3/2}/l$. Since both K and l approach zero at the wall, the boundary condition for ε is undefined. The ε equation is solved only in a reduced domain excluding the same as previous investigators Fraikin[12] and Ozoe et al.[13], thus

$$\varepsilon_1=(C_\mu^{3/4}K_l^{3/2})/(\chi\Delta_1) \quad (20)$$

where subscript 1 denotes the nearest grid point from the wall, x is Von Karman's constant having

a value of 0.42 and Δ_1 is the dimension of the first node from the wall.

The horizontal upper and lower walls are conducting wall, and then the vertical hot and cold walls are zero-thickness, non-conduction wall and constant temperature wall.

3. Numerical Analysis

The standard k-ε model turbulent governing equations have been solved by the finite volume calculation procedure including SIMPLE(Semi-Implicit Method for Pressure Linked Equations) algorithm[15] which is developed using control volumes and staggered grids, the power law scheme, and TDMA (Tri-Diagonal Matrix Algorithm).

In order to improve convergence, the under relaxation factors of velocity, pressure, temperature, K, ε and μ_t are applied 0.01, 0.03, 0.05, 0.02, 0.02 and 0.05, respectively. A grid distribution in the x and y direction is 64 and 42, respectively. The grids were tested for some selected situation (54×32, 64×42, 72×42 and 72×52). It was found that the grid dependency on the calculated results was within 5% as a whole. The grid node near the four walls is distributed into a denser node than that of core region. The converged solutions are obtained when the error of energy balance is less than 0.01% and such that;

$$\left| \frac{\phi^{m+1} - \phi^{m}}{\phi^{m}} \right| < 10^{-3} \qquad (21)$$

The numerical results are compared with the measured values of a operating PWR plant to verify the analysis program[7, 8]. The plant data of Lubin[7, 8] were made for a reactor coolant system line of typical CE type in a light water nuclear reactor. This data, taken from an operating plant, consists of horizontal run of about 4.9m between two valves. The horizontal line is a 0.333m, schedule 160 stainless steel line, with an inner diameter of 0.267m and wall thickness 0.033m. The ambient environment is 38℃ and the line is insulated with an equivalent heat transfer coefficient of about 0.026 W/m^{2}K.

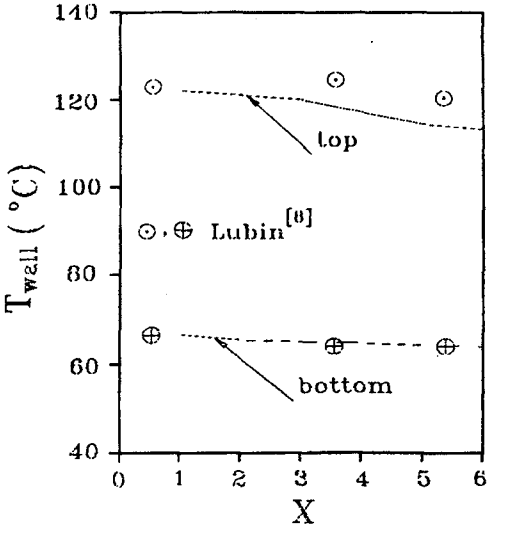

Fig. 3. Comparison Between Plant Test and our Analysis Data(at T_{hot}=149℃ and T_{cold}=38℃)

This comparison is shown in Fig. 3. The numerical results are shown to agree well with the plant measured data except for small discrepancies near the top wall.

4. Result and Discussion

The design specification of safety injection tank line for the numerical analysis is shown in the Table 2 (ASME and ASTM A376 Gr TP316), in which the heat transfer coefficient is for the insulated pipe. All properties are calculated by the harmonic mean temperature of cold and hot fluid.

Under the above condition, the dimensionless variables are G_r=1.74×10^{11}, Pr=1.91 and Bi=4.82×10^{-5}, and the other variables are T_∞ =0.0, a=0.1, k_s/k_f=22.3. In this study, the

Table 2. Design Spec. of Safety Injection Tank Line

Properties & Spec.	Value
I.D of pipe	0.284 m
Thickness of pipe	0.028 m
Material of pipe	SA-312-TP-347
Conductivity	15.1 W/m K
Heat transfer coef.	0.026 W/m^2 K
Ambient temp.	38 ℃

numerical analysis was carried out for the above conditions

4.1. The Dimensionless Distribution of Physical Quantities

The dimensionless distribution of isotherms, streamlines, turbulent kinetic energy and turbulent viscosity for the in case of standard calculation are shown in Fig. 4. The bracket in the Fig.4 denotes [minimum value (interval) maximum value] of the variables.

In Fig. 4(a)(b), it is shown that thermal stratified flow occurs in the pipe line at the Biot number of 4.82×10^{-5}, i.e., hotter fluid flows the upper portion of the pipe line and colder fluid flows the lower portion of the pipe line. Heat is transferred through the top (hotter) intrusion layer and by conduction in the y-direction (circumferential direction) to the lower section of the pipe line, where it is then transferred to the bottom (cooler) intrusion layer.

The distribution of dimensionless turbulent kinetic energy, K, and turbulent viscosity, μ_t, are shown in Fig.4 (c), (d). We can show from this figure that the turbulent quantities(K and μ_t) of the core regions are not appear but only strongly appear near the hot and cold wall. This means that the turbulent flow exists to only the hot and cold wall regions and the remain regions(almost core) does not exist turbulent flow, i.e, stationary flow.

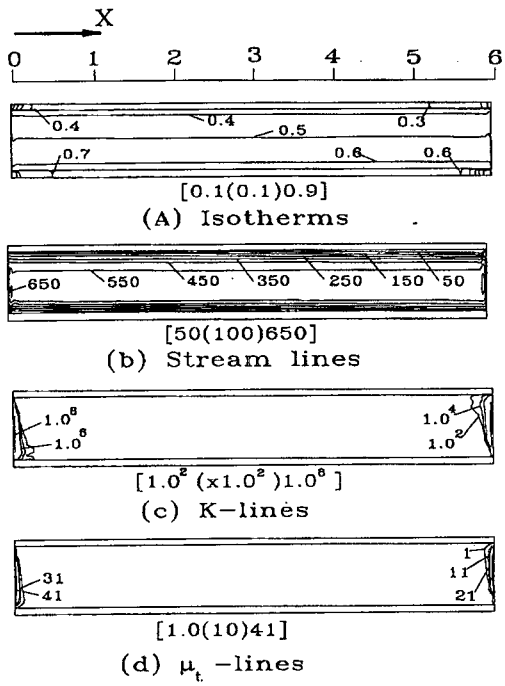

Fig. 4. The Distribution of (a)Isotherms, (b)Streamlines, (c)Turbulent Kinetic Energy and (d)Turbulent Viscosity ($Gr=1.74\times10^{11}$, $Pr=1.91$, $Bi=4.82\times10^{-5}$, $k_s/k_f=22.3$ and $a=0.1$)

4.2. The Effect of Heat Transfer Rates of Pipeline

Fig. 5 shows the temperature distribution of pipe wall at the selected axial distance (x=3). This temperature distributions are calculated by the assumption that those of fluid are a function of circumferential direction(y-direction) because the temperature distribution at the same level is nearly equalized by the thermal stratification in the enclosures. The angular variation in wall temperature is the consequence of pipe wall conduction in the circumferential direction around the wall. The local variation in fluid temperatures

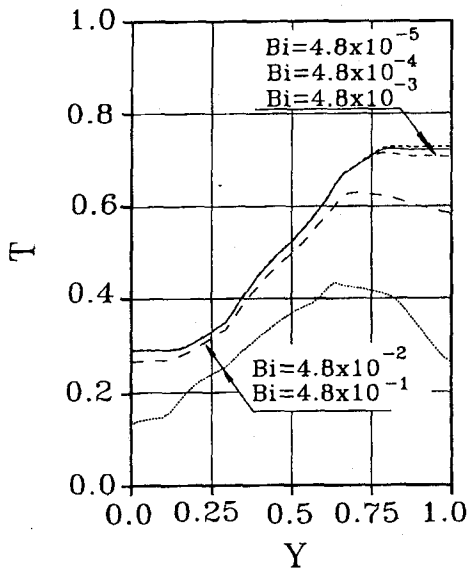

Fig. 5. The Temperature Distribution for y Direction for Various Biot Numbers at x=3 ($Gr=1.74\times10^{11}$, $Pr=1.91$, $k_s/k_f=22.3$ and $a=0.1$)

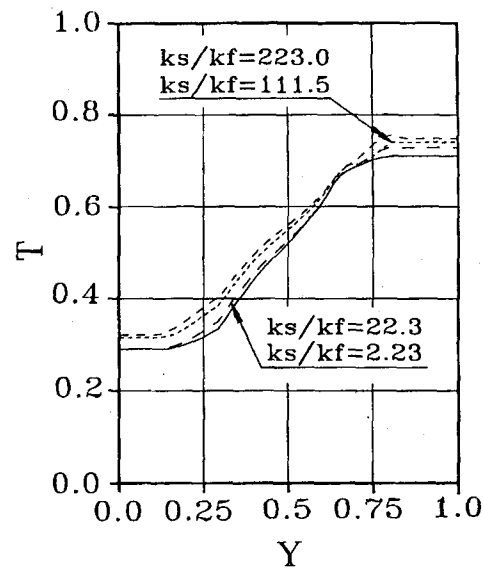

Fig. 6. Temperature Distribution for y Direction for Various Thermal Conductivities at x=3 ($Gr=1.74\times10^{11}$, $Pr=1.91$, $Bi=4.82\times10^{-5}$ and $a=0.1$)

will not appreciably alter the intrusion layer flow pattern. It is known that the wall temperature between top and bottom of pipe significantly reduces as the heat transfer rate at the pipe wall increases, because of the mixing effect by natural convection. The results show that the thermal stratification exists in the pipe; however, a significant reduction of the temperature difference of pipe wall from top to bottom can be observed over the Biot number of 4.82×10^{-1}.

So, the thermal stress of the pipe wall may be reduced significantly. Therfore, as a result, the heat transfer coefficient of outside surface in pipe should be increased in order to significantly reduce the thermal stratification phenomenon. In case of the Biot number of 4.82×10^{-1} of the Fig. 5, we can show that the temperature of inside fluid is hotter than that of the outside wall between y=0.75 and y=1.0. This means that the heat flux of outside surface in pipe is more than that of inside fluid because of the large heat transfer rates of pipeline wall.

4.3. The Effect of Thermal Conductivity of Wall Pipeline

In order to see if the thermal conductivity of the wall pipeline might effect thermal stratification, the analysis is done only for the variation of thermal conductivity of pipeline with other fixed conditions. The dimensionless distribution of physical quantities for the variation of the thermal conductivity are similar to that shown in Fig. 4. It is shown that the pattern of physical quantities is nearly not changed even if the thermal conductivity of pipeline increases. Also, as shown in Fig. 6, the temperature difference between top and bottom of pipe circumference direction is

nearly not changed even if the thermal conductivity of pipeline increases. The results show that the increase of the thermal conductivity of the wall weakens a little the thermal stratification and somewhat reduces temperature gradient of y-direction in the pipe wall. These effects are however minor, when compared with those due to the variation of the heat transfer rates at the surface of the pipe wall.

4.4. The Effect of Pipeline Wall Thickness

In order to see if the thickness of the pipeline might effect thermal stratification; also, the analysis is performed only for the variation of pipeline thickness with other all fixed conditions. The dimensionless distribution of physical quantities for the variation of the wall thickness are nearly similar to that shown in Fig. 4. It is shown that the pattern of physical quantities is nearly not changed even if the thickness of pipeline increases. However, as shown in Fig. 7, the temperature difference between top and bottom of pipe circumference somewhat reduces as the thickness of pipeline increases between y=0.5 and y=0.8 due to conduction effect through the wall. The results show that the increase of the wall thickness of the wall weakens a little the thermal stratification and somewhat reduces temperature gradient of y-direction in the pipe wall. These effects are however minor, when compared with those due to the variation of the heat transfer rates at the surface of the pipe wall.

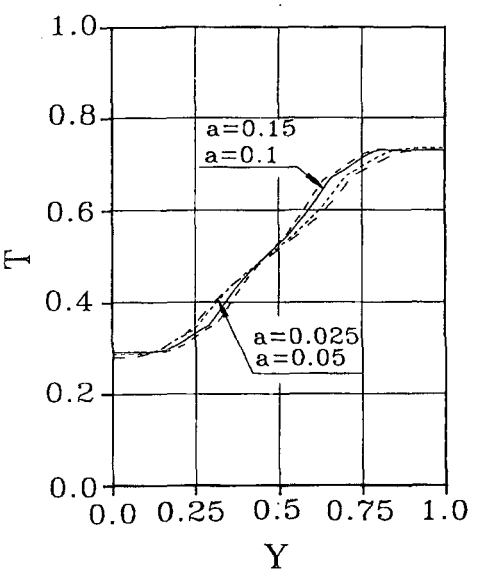

Fig. 7. The Temperature Distribution for y Direction for Various Wall Thickness at x=3.($Gr=1.74\times10^{11}$, Pr=1.91, ks/kf = 22.3 and $Bi=4.82\times10^{-5}$)

5. Conclusions

This study have been performed for the heat transfer and flow characteristics in a long horizontal line (the safety injection line) with different end temperatures undergoing natural convection at very high Rayleigh number. From this study, we obtain the following conclusions:

The results show that the heat transfer rate at the pipe surface is the controlling parameter which can reduce thermal stratification in the pipeline and that the thermal stratification occurs at the Biot number of 4.82×10^{-1} which corresponds to the design and environmental conditions of the safety injection line of the PWR plant. A significant reduction and, eventually, the disappearance of the phenomenon are observed over the Biot number of 4.82×10^{-1}.

The results also show that the increase of the thermal conductivity and the thickness of the wall weakens the thermal stratification and reduces temperature gradient of y-direction in the pipe wall, but their influence is less pronounced than that due to the variation of the heat transfer rates at the surface of the pipe wall. Therefore, the increase of heat transfer rate at the surface of the

pipe is a major factor to prevent thermal stratification of the flow in the safety injection line connected with the RCS main pipe line of the PWR plant.

Nomenclature

a : thickness ratio of pipe
B : buoyancy term
B_i : Biot number
C_1, C_2, C_3, C_μ : empirical turbulence model constants
G_r : Grashof number
h : heat transfer coefficient
H : length from top to bottom
k : thermal conductivity
K : turbulent kinetic energy
L : length from left to right
P : pressure
P_r : Prandtl number
T : temperature
u,v : velocities in the x and y directions
x,y : cartesian coordinate
β : coefficient of thermal expansion
χ : Von Karman' s Constant
Γ : exchange coefficient
Δ_1: dimension of the first node from the wall
ϵ : dissipation rate of turbulent kinetic energy
μ : molecular viscosity
μ_t : turbulent viscosity
σ_K, σ_T, σ_ϵ : turbulent Prandtl number for K, T and ϵ
ν : kinematic viscosity
ϕ : general dependent variable

Subscripts

hot, cold : hot and cold regions
f : fluid regions
s : solid regions, surface regions
∞ : environment
eff : effective value

Superscripts

m : iteration number
* : physical quantity

References

1. NRC, "Thermal Stress in Piping Connected to RCS", NRC *Bulletin No. 88-08*, (1988).
2. NRC, "Pressurizer Surge Line Thermal Stratification", NRC Bulletin No. 88-11, (1988).
3. Hong, S. W., "Natural Circulation in Horizontal Pipe", *Int. J. of Heat and Mass Transfer*, Vol.20, pp. 685-691, (1977).
4. Bejan, A. and C. L. Tien, "Fully Developed Natural Counterflow in a Long Horizontal Pipe with Different End Temperatures", *Int. J. of Heat and Mass Transfer*, Vol.21, pp. 701-708, (1978).
5. Kimura, S., and Bejan, A., "Experimental Study of Natural Convection in a Horizontal Cylinder with Different End Temperatures", *Int. J. Heat and Mass Transfer*, Vol.23, pp. 1117-1126, (1980).
6. Shiralkar, G., Gadgh, A., and Tien, C. L., "High Rayleigh Number Convection in Shallow Enclosures with Different End Temperatures", *Int. J. Heat and Mass Transfer*, Vol. 24 , pp. 1621-1629, (1981).
7. Lubin, B. T., and Kim, J. H., "Prediction of Wall Temperatures in Long Lines Under-going Natural Convection at High Rayleigh Numbers", *IHTC-10, International Heat Transfer Conference*, Brighton, UK, 12-NM-20, pp.519-524, (1994).
8. Lubin, B.T. and Brown, J., "Thermal Stratification in Lines Connected to a Reactor Coolant System", *Int. Pressure Vessels and Piping Codes and Standards*, PVP-Vol. 313-1, pp. 19-31, (1995).
9. Farouk, B., Laminar and "Turbulent Natural

Convection Heat Transfer from Horizontal Cylinders", *Ph. D Thesis Univ. of Delaware.* (1981).

10. Park, M. H. and Lee, J. H, "Turbulent Natural Convection Flow and Heat Transfer in an Inclined Square Enclosure", *KSME J.*, Vol.6 No.1, pp. 16-23, (1992).
11. Paolucci, S. and Chenoweth, D. R., "Natural Convection in Shallow Enclosures with Differentially Heated End Walls", *Int. J. Heat and Mass Transfer,* Vol. 110, pp. 625-634, (1988).
12. Launder, B.E. and Spalding, D. B., "The Numerical Computation of Turbulent Flows", *Computer Methods in Applied Mechanics and Engineering*, 3, pp.269-298, (1974).
13. Fraikin. M. P., Portier. J. J. and Frailkin C. J. "Application of k-ϵ Turbulence Model to an Enclosure Buoyance Driven Recirculation Flows", *ASME Paper No. 80-MT-68*, July, pp.1-12, (1980).
14. Ozoe. H, Mouri. A., Ohmuro. M., Churchill S. W. and Lior. N, "Numerical Calculation of Laminar and Turbulent Natural Convection in Water in Rectangular Channels Heated and Cooled Isothermally on the Opposing Vertical Walls", *Int. T. Heat Transfer Vol.18, No.1* pp. 125-138, (1985).
15. Patankar, S. V., *"Numerical Heat Transfer and Fluid Flow"*, McGraw-Hill Book Company, (1980).